

# Bis(amido)ruthenium(IV) Complexes with 2,3-Diamino-2,3-dimethylbutane. Crystal Structure and Reversible Ru(IV)–Amide/Ru(III)–Amine and Ru(IV)–Amide/Ru(II)–Amine Redox Couples in Aqueous Solution

Wing-Hong Chiu, Shie-Ming Peng,<sup>†</sup> and Chi-Ming Che\*

Department of Chemistry, The University of Hong Kong, Pokfulam Road, Hong Kong

Received September 1, 1995<sup>⊗</sup>

Two bis(amido)ruthenium(IV) complexes,  $[\text{Ru}^{\text{IV}}(\text{bpy})(\text{L}-\text{H})_2]^{2+}$  and  $[\text{Ru}^{\text{IV}}(\text{L})(\text{L}-\text{H})_2]^{2+}$  (bpy = 2,2'-bipyridine, L = 2,3-diamino-2,3-dimethylbutane, L-H =  $(\text{H}_2\text{NCMe}_2\text{CMe}_2\text{NH}^-)$ ), were prepared by chemical oxidation of  $[\text{Ru}^{\text{II}}(\text{bpy})(\text{L})_2]^{2+}$  and the reaction of  $[(n\text{-Bu})_4\text{N}][\text{Ru}^{\text{VI}}\text{NCl}_4]$  with L, respectively. The structures of  $[\text{Ru}(\text{bpy})(\text{L}-\text{H})_2][\text{ZnBr}_4]\cdot\text{CH}_3\text{CN}$  and  $[\text{Ru}(\text{L})(\text{L}-\text{H})_2]\text{Cl}_2\cdot 2\text{H}_2\text{O}$  were determined by X-ray crystal analysis.  $[\text{Ru}(\text{bpy})(\text{L}-\text{H})_2][\text{ZnBr}_4]\cdot\text{CH}_3\text{CN}$  crystallizes in the monoclinic space group  $P2_1/n$  with  $a = 12.597(2)$  Å,  $b = 15.909(2)$  Å,  $c = 16.785(2)$  Å,  $\beta = 91.74(1)^\circ$ , and  $Z = 4$ .  $[\text{Ru}(\text{L})(\text{L}-\text{H})_2]\text{Cl}_2\cdot 2\text{H}_2\text{O}$  crystallizes in the tetragonal space group  $I4_1/a$  with  $a = 31.892(6)$  Å,  $c = 10.819(3)$  Å, and  $Z = 16$ . In both complexes, the two Ru–N(amide) bonds are *cis* to each other with bond distances ranging from 1.835(7) to 1.856(7) Å. The N(amide)–Ru–N(amide) angles are about  $110^\circ$ . The two Ru(IV) complexes are diamagnetic, and the chemical shifts of the amide protons occur at around 13 ppm. Both complexes display reversible metal–amide/metal–amine redox couples in aqueous solution with a pyrolytic graphite electrode. Depending on the pH of the media, reversible/quasireversible  $1\text{e}^- - 2\text{H}^+$  Ru(IV)–amide/Ru(III)–amine and  $2\text{e}^- - 2\text{H}^+$  Ru(IV)–amide/Ru(II)–amine redox couples have been observed. At pH = 1.0, the  $E^\circ$  is 0.46 V for  $[\text{Ru}^{\text{IV}}(\text{bpy})(\text{L}-\text{H})_2]^{2+}/[\text{Ru}^{\text{III}}(\text{bpy})(\text{L})_2]^{3+}$  and 0.29 V vs SCE for  $[\text{Ru}^{\text{IV}}(\text{L})(\text{L}-\text{H})_2]^{2+}/[\text{Ru}^{\text{III}}(\text{L})_3]^{3+}$ . The difference in the  $E^\circ$  values for the two Ru(IV)–amide complexes has been attributed to the fact that the chelating saturated diamine ligand is a better  $\sigma$ -donor than 2,2'-bipyridine.

## Introduction

The oxidation chemistry of high-valent ruthenium complexes containing metal–ligand multiple bonds has attracted much attention in recent years.<sup>1,2</sup> However, despite the very rich oxidation chemistry of Ru=O complexes,<sup>1–3</sup> studies on high-valent ruthenium–nitrido,<sup>1,4</sup> –amido,<sup>1,5</sup> and –imido<sup>1,6</sup> complexes are sparse. For high-valent ruthenium– and osmium–oxo complexes, reversible proton-coupled multielectron transfer reactions have been observed in aqueous solutions, for example the reversible two-proton two-electron  $\text{Ru}^{\text{VI}}\text{O}_2/\text{Ru}^{\text{IV}}\text{O}(\text{OH})_2^{1-3}$

and three-proton three-electron  $\text{Os}^{\text{VI}}\text{O}_2/\text{Os}^{\text{III}}(\text{OH})(\text{OH})_2^7$  couples. We<sup>8</sup> and Meyer<sup>9</sup> and co-workers have also studied the proton-coupled electrochemical reduction of  $\text{Os}^{\text{VI}}\equiv\text{N}$  to  $\text{Os}^{\text{III}}-\text{NH}_3$  in aqueous solution. However, owing to the large kinetic barrier involved in oxidative deprotonation of  $\text{Os}^{\text{III}}-\text{NH}_3$ , the  $\text{Os}^{\text{VI}}\equiv\text{N}/\text{Os}^{\text{III}}-\text{NH}_3$  couple is not reversible. Prior to our previous reports on the redox chemistry of ruthenium<sup>6b</sup> and osmium<sup>10</sup> complexes of 2,3-diamino-2,3-dimethylbutane (L), there were no reports on reversible metal–amide/metal–amine and metal–imide/metal–amine redox couples in aqueous solution. Sargeson and co-workers noted that oxidative deprotonation of  $[\text{Ru}(\text{sar})]^{2+}$  (sar = 3,6,10,13,16,19-hexaazabicyclo[6.6.6]icosane) to a Ru<sup>II</sup>-imine species proceeded through a short-lived ruthenium(IV)–imido intermediate.<sup>11</sup> This species, which was characterized by UV–vis absorption spectroscopy, was suggested to undergo rapid intramolecular ligand oxidative deprotonation leading to the formation of Ru(II)–imine species. We anticipate that, with the use of primary and secondary amines containing no  $\alpha$ -CH groups, such a reaction could be prohibited and thus the isolation of high-valent ruthenium–amido and –imido complexes would become feasible. In our earlier communication, the complex  $[\text{Ru}(\text{bpy})_2(\text{L})](\text{ClO}_4)_2$  (**1**) (bpy = 2,2'-bipyridine) was reported.<sup>6b</sup> The title ligand was chosen because it contains no  $\alpha$ -CH group. The electrochemistry of **1** was found to be reminiscent of that of ruthenium–oxo complexes<sup>1b</sup> in that a reversible proton-coupled Ru–imide/Ru–amine redox couple has been observed

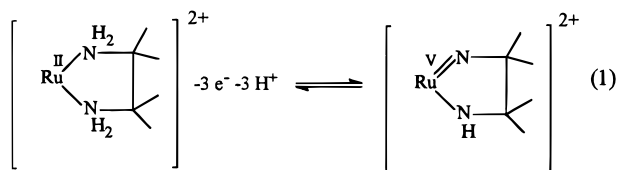
<sup>†</sup> Present address: National Taiwan University.

<sup>⊗</sup> Abstract published in *Advance ACS Abstracts*, May 1, 1996.

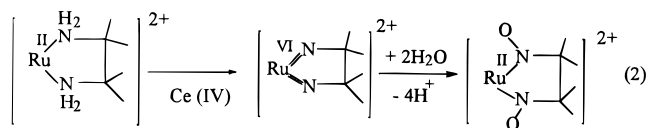
- (1) (a) Che, C. M. *Pure Appl. Chem.* **1995**, *67*, 225. (b) Che, C. M.; Yam, V. W. W. *Adv. Inorg. Chem.* **1992**, *39*, 233.
- (2) Griffith, W. P. *Chem. Soc. Rev.* **1992**, 179.
- (3) (a) Dovletoglou, A.; Meyer, T. J. *J. Am. Chem. Soc.* **1994**, *116*, 215. (b) Adeyemi, S. A.; Dovletoglou, A.; Meyer, T. J. *Inorg. Chem.* **1992**, *31*, 1375.
- (4) (a) Griffith, W. P. *Coord. Chem. Rev.* **1972**, *8*, 370. (b) Griffith, W. P.; Pawson, D. J. *Chem. Soc., Dalton Trans.* **1973**, 1315. (c) Pawson, D.; Griffith, W. P. *J. Chem. Soc., Dalton Trans.* **1975**, 417. (d) Schwab, J. J.; Wilkinson, E. C.; Wilson, S. R.; Shapley, P. A. *J. Am. Chem. Soc.* **1991**, *113*, 6124.
- (5) (a) Che, C. M.; Cheng, W. K.; Leung, W. H.; Mak, T. C. W. *J. Chem. Soc., Chem. Commun.* **1987**, 418. (b) Huang, J. S.; Li, Z. Y.; Poon, C. K.; Che, C. M. *Inorg. Chem.* **1992**, *31*, 1313. (c) Adcock, P. A.; Keene, F. R.; Smythe, R. S.; Snow, M. R. *Inorg. Chem.* **1984**, *23*, 2336. (d) Redshaw, C.; Clegg, W.; Wilkinson, G. J. *Chem. Soc., Dalton Trans.* **1992**, 2059.
- (6) (a) Huang, J. S.; Che, C. M.; Poon, C. K. *J. Chem. Soc., Chem. Commun.* **1992**, 161. (b) Wong, K. Y.; Che, C. M.; Li, C. K.; Chiu, W. H.; Zhou, Z. Y.; Mak, T. C. W. *J. Chem. Soc., Chem. Commun.* **1992**, 754. (c) Chiu, W. H.; Cheung, K. K.; Che, C. M. *J. Chem. Soc., Chem. Commun.* **1995**, 441. (d) Kee, T. P.; Park, L. Y.; Robbins, J.; Shrock, R. R. *J. Chem. Soc., Chem. Commun.* **1991**, 121. (e) Danopoulos, A. A.; Wilkinson, G.; Bilquis, H.-B.; Hursthouse, M. B. *Polyhedron* **1992**, 2961. (f) Toozee, R. P.; Wilkinson, G.; Motevall, M.; Hursthouse, M. B. *J. Chem. Soc., Dalton Trans.* **1986**, 2711. (g) Shapley, P. A.; Kim, H. S.; Wilson, S. R. *Organometallics* **1988**, *7*, 928.

- (7) (a) Che, C. M.; Cheng, W. K.; Yam, V. W. W. *J. Chem. Soc., Dalton Trans.* **1990**, 3095. (b) Dobson, J. C.; Takeuchi, K. J.; Pipes, D. W.; Geselowitz, D. A.; Meyer, T. J. *Inorg. Chem.* **1986**, *25*, 2357.
- (8) Che, C. M.; Wong, K. Y.; Lam, H. W.; Chin, K. F.; Zhou, Z. Y.; Mak, T. C. W. *J. Chem. Soc., Dalton Trans.* **1993**, 857.
- (9) Coia, G. M.; White, P. S.; Meyer, T. J.; Wink, D. A.; Keefer, L. K.; Davis, W. M. *J. Am. Chem. Soc.* **1994**, *116*, 3649.
- (10) Chin, K. F.; Wong, K. Y.; Che, C. M. *J. Chem. Soc., Dalton Trans.* **1993**, 197.
- (11) Bernhard, B.; Sargeson, A. M. *J. Am. Chem. Soc.* **1989**, *111*, 597.

in aqueous solution (eq 1). However the proposed Ru(V)–



imido intermediate (eq 1)<sup>6b</sup> is stable on the time scale of cyclic voltammetry only. During isolation, the ligand L was cleaved into two imine groups, and  $[\text{Ru}(\text{bpy})_2(\text{HN}=\text{CMe}_2)_2]^{2+}$  resulted. Subsequent studies showed that oxidation of **1** by ammonium cerium(IV) nitrate gave  $[\text{Ru}^{\text{II}}(\text{bpy})_2(\text{ONC}(\text{Me})_2\text{C}(\text{Me})_2\text{NO})]^{2+}$ ,<sup>6c</sup> the formation of which was suggested to come from a reactive bis(imido)ruthenium(VI) (eq 2).



Thus, even with this chelating ligand, the cationic ruthenium–imido complexes derived are still very reactive. Thus, we turned our study to the ruthenium–amido complexes.

Herein are described the syntheses and electrochemistry of the two Ru(II)–amine complexes  $[\text{Ru}^{\text{II}}(\text{bpy})(\text{L})_2]^{2+}$  and  $[\text{Ru}^{\text{II}}(\text{L})_3]^{2+}$  and the crystal structures of the two bis(amido)ruthenium(IV) complexes  $[\text{Ru}^{\text{IV}}(\text{bpy})(\text{L}-\text{H})_2][\text{ZnBr}_4] \cdot \text{CH}_3\text{CN}$  and  $[\text{Ru}^{\text{IV}}(\text{L})(\text{L}-\text{H})_2]\text{Cl}_2 \cdot 2\text{H}_2\text{O}$  (L-H =  $(\text{H}_2\text{NCMe}_2\text{CMe}_2\text{NH})^-$ ).

## Experimental Section

**Materials.**  $[(n\text{-Bu})_4\text{N}][\text{RuNCl}_4]$ ,<sup>4b</sup> 2,3-diamino-2,3-dimethylbutane (L),<sup>12</sup> and  $\text{Ru}(\text{bpy})\text{Cl}_3$ <sup>13</sup> were prepared according to the published methods. Acetonitrile (Mallinckrodt, chromAR, HPLC grade) was twice distilled over  $\text{CaH}_2$  and  $\text{KMnO}_4$ . All other reagents and solvents used in syntheses and physical measurements were of analytical grade.

**Instrumentation and Techniques.** UV–vis spectra were obtained on a Shimadzu UV-240 spectrophotometer. NMR spectra were run on a JEOL 270 multinuclear FT-NMR spectrometer, and chemical shifts were referenced to TMS. Infrared spectra were obtained as Nujol mulls on a Nicolet 20 SXC FT-IR spectrophotometer. Elemental analyses were performed by Butterworth Co. Ltd.

Cyclic voltammetry and controlled-potential coulometry were performed by using a Princeton Applied Research (PAR) Model 175 universal programmer, Model 173 potentiostat, and Model 179 digital coulometer. The working electrode used was edge plane pyrolytic graphite (EPG, Union Carbide). The electrode surfaces were pretreated by procedures as previously described.<sup>14</sup>

**Preparation of Complexes.  $[\text{Ru}^{\text{II}}(\text{bpy})(\text{L})_2][\text{ZnCl}_4]$  (**2**).** Ligand L (0.3 g) and  $\text{Ru}(\text{bpy})\text{Cl}_3$  (0.2 g) were added to absolute ethanol (50 mL). Zinc dust (1.4 g) was added, and the mixture was heated at reflux for 6 h. The solution was cooled and was filtered to remove zinc dust. Hydrochloric acid (0.2 M, 10 mL) was added, and the solvent was reduced by rotary evaporation to about 10 mL. The orange solid was collected and washed with water and then diethyl ether (yield 80%). Anal. Calcd for  $[\text{RuC}_{22}\text{H}_{40}\text{N}_6][\text{ZnCl}_4]$ : C, 37.91; H, 5.74; N, 12.06. Found: C, 38.10; H, 5.53; N, 11.96.

**$[\text{Ru}^{\text{II}}(\text{bpy})(\text{L})_2](\text{PF}_6)_2$  (**3**).** This was prepared by a procedure similar to that for **2** except a saturated solution of ammonium hexafluorophosphate (10 mL) was used instead of hydrochloric acid (yield 85%). Anal. Calcd for  $[\text{RuC}_{22}\text{H}_{40}\text{N}_6](\text{PF}_6)_2$ : C, 33.89; H, 5.13; N, 10.78. Found: C, 33.72; H, 5.58; N, 10.97. IR:  $\nu(\text{N}-\text{H})$  3308 and 3280  $\text{cm}^{-1}$ . UV–vis in  $\text{CH}_3\text{CN}$  [ $\lambda_{\text{max}}/\text{nm}$  ( $\epsilon_{\text{max}}/\text{mol}^{-1} \text{dm}^3 \text{cm}^{-1}$ )]: 246 (12 080), 296

(22 800), 372 (6150), 518 (4060). FABMS ( $m/e$ ): 634  $[\text{M} - \text{PF}_6]^+$ . <sup>1</sup>H and <sup>13</sup>C NMR data for  $[\text{Ru}^{\text{II}}(\text{bpy})(\text{L})_2](\text{PF}_6)_2$  in  $\text{CD}_3\text{CN}$  are as follows. Aromatic protons: 9.44 (d, 2H), 8.45 (d, 2H), 7.91 (t, 2H), 7.53 ppm (t, 2H). Amine protons: 5.21, 3.99, 3.88, 3.68 ppm (d, 8H). Methyl protons: 1.47, 1.35, 1.21, 1.09 ppm (s, 24H). Aromatic carbons: 162.15, 156.08, 135.15, 126.00, 123.72 ppm. Quaternary carbons: 64.56, 60.77 ppm. Methyl carbons: 26.79, 25.84, 25.29, 24.88 ppm.

**$[\text{Ru}^{\text{IV}}(\text{bpy})(\text{L}-\text{H})_2](\text{PF}_6)_2$  (**4**).** Complex **3** (0.1 g) was dissolved in acetonitrile (10 mL); then a bromine solution (5 drops of liquid bromine in 10 mL of  $\text{CH}_3\text{CN}$ ) was added slowly. The solution was stirred at room temperature overnight, the solvent was removed by rotary evaporation, and the residue was dissolved in  $\text{CH}_3\text{CN}$  (1 mL). Then diethyl ether was added to give the yellow product, which was collected, washed with diethyl ether, and air-dried (yield 85%). This could be recrystallized by diffusion of diethyl ether into an acetonitrile solution. Complex **4** could also be prepared by electrochemical oxidation of **3** at 0.60 V vs SCE in 0.1 M  $\text{CF}_3\text{COOH}$ . The solid was precipitated by addition of  $\text{NH}_4\text{PF}_6$  after electrolysis (yield 30%). Anal. Calcd for  $[\text{RuC}_{22}\text{H}_{38}\text{N}_6](\text{PF}_6)_2$ : C, 33.98; H, 4.89; N, 10.81. Found: C, 33.77; H, 4.77; N, 10.90. IR:  $\nu(\text{N}-\text{H})$  3302, 3196.4  $\text{cm}^{-1}$ . UV–vis in  $\text{CH}_3\text{CN}$  [ $\lambda_{\text{max}}/\text{nm}$  ( $\epsilon_{\text{max}}/\text{mol}^{-1} \text{dm}^3 \text{cm}^{-1}$ )]: 245 (15 170), 286 (13 820) br, 310.9 (10 770) sh, 415 (5540) br. FABMS ( $m/e$ ): 633  $[\text{M} - \text{PF}_6 + \text{H}]^+$ , 487  $[\text{M} - 2\text{PF}_6]^+$ . <sup>1</sup>H and <sup>13</sup>C NMR data for  $[\text{Ru}^{\text{IV}}(\text{bpy})(\text{L}-\text{H})_2](\text{PF}_6)_2$  in  $\text{CD}_3\text{CN}$  are as follows. Aromatic protons: 9.48 (d, 2H), 8.55 (d, 2H), 8.29 (t, 2H), 7.78 ppm (t, 2H). Amine protons: 13.16 (s, NH, 2H), 4.69 (d,  $\text{NH}_2$ , 2H), 3.13 ppm (d,  $\text{NH}_2$ , 2H). Methyl protons: 1.47, 1.10, 0.99, 0.52 ppm (s, 24H). Aromatic carbons: 155.00, 153.12, 142.21, 128.06, 124.78 ppm. Quaternary carbons: 79.38, 62.91 ppm. Methyl carbons: 25.88, 25.72, 24.60, 20.31 ppm.

**$[\text{Ru}^{\text{IV}}(\text{bpy})(\text{L}-\text{H})_2][\text{ZnBr}_4]$  (**5**).** This was prepared from **2** by a procedure similar to that for **4** (yield 75%). Anal. Calcd for  $[\text{RuC}_{22}\text{H}_{38}\text{N}_6][\text{ZnBr}_4]$ : C, 30.28; H, 4.36; N, 9.63. Found: C, 30.46; H, 4.28; N, 9.53.

**$[\text{Ru}^{\text{II}}(\text{L})_3](\text{PF}_6)_2$  (**6**).** Ligand L (0.14 g) was dissolved in degassed water (10 mL), and a mixture of  $\text{RuCl}_3 \cdot x\text{H}_2\text{O}$  (0.1 g) and zinc dust (0.4 g) was added under an argon atmosphere. The solution mixture was heated at reflux for 4 h, cooled to room temperature, and filtered under an argon atmosphere. A yellow solid was precipitated upon addition of  $\text{NH}_4\text{PF}_6$ . The product was recrystallized by diffusion of diethyl ether into a degassed acetone solution (yield 70%). Anal. Calcd for  $[\text{RuC}_{18}\text{H}_{48}\text{N}_6](\text{PF}_6)_2$ : C, 29.23; H, 6.50; N, 11.37. Found: C, 29.10; H, 6.30; N, 11.27. IR:  $\nu(\text{N}-\text{H})$  3340, 3296  $\text{cm}^{-1}$ . UV–vis in 0.1 M  $\text{CF}_3\text{COOH}$  [ $\lambda_{\text{max}}/\text{nm}$  ( $\epsilon_{\text{max}}/\text{mol}^{-1} \text{dm}^3 \text{cm}^{-1}$ )]: 271 (900), 402.4 (300). <sup>1</sup>H NMR data for  $[\text{Ru}^{\text{II}}(\text{L})_3](\text{PF}_6)_2$  in  $\text{CD}_3\text{CN}$  are as follows. Methyl protons: 1.23 ppm (s, 36 H). Amine protons: 3.15 ppm (s, 12H).

**$[\text{Ru}^{\text{IV}}(\text{L})(\text{L}-\text{H})_2]\text{Cl}_2$  (**7**).** A solution of  $[\text{n-Bu}_4\text{N}][\text{Ru}^{\text{VI}}\text{NCl}_4]$  (0.1 g) and ligand L (0.1 g) in acetone (10 mL) was stirred for 12 h at room temperature. The red solid precipitate was filtered off and washed with diethyl ether. It was recrystallized by diffusion of diethyl ether into a methanolic solution (yield 75%). Anal. Calcd for  $[\text{RuC}_{18}\text{H}_{46}\text{N}_6]\text{Cl}_2 \cdot 2\text{H}_2\text{O}$ : C, 38.99; H, 9.03; N, 15.16. Found: C, 39.12; H, 8.58; N, 14.96. IR:  $\nu(\text{N}-\text{H})$  3328, 3205, 3120  $\text{cm}^{-1}$ . UV–vis in MeOH [ $\lambda_{\text{max}}/\text{nm}$  ( $\epsilon_{\text{max}}/\text{mol}^{-1} \text{dm}^3 \text{cm}^{-1}$ )]: 305 (3500) sh, 408 (860) sh. FABMS ( $m/e$ ): 519  $[\text{M} + \text{H}]^+$ , 483  $[\text{M} - \text{Cl}]^+$ , 448  $[\text{M} - 2\text{Cl}]^+$ . <sup>1</sup>H and <sup>13</sup>C NMR data for  $[\text{Ru}^{\text{IV}}(\text{L})(\text{L}-\text{H})_2]\text{Cl}_2$  in  $\text{CDCl}_3$  and methanol-*d*<sub>4</sub>, respectively, are as follows. Amine protons: 12.31 (s, NH, 2H), 7.51, 5.97, 2.94, 2.13 ppm (d,  $\text{NH}_2$ , 8H). Methyl protons: 1.27, 1.25, 1.21, 1.19, 1.18, 0.92 ppm (s, 36H). Quaternary carbons: 76.63, 63.38, 61.78 ppm. Methyl carbons: 26.42, 25.67, 25.55, 24.83, 24.69, 24.39 ppm.

**Crystal Structure Determination.** The details of crystal data collection and refinement parameters of  $[\text{Ru}(\text{bpy})(\text{L}-\text{H})_2][\text{ZnBr}_4] \cdot \text{CH}_3\text{CN}$  and  $[\text{Ru}(\text{L})(\text{L}-\text{H})_2]\text{Cl}_2 \cdot 2\text{H}_2\text{O}$  are listed in Table 1. All diffraction data were collected on an Enraf-Nonius CAD4 diffractometer using the  $\theta$ – $2\theta$  scan mode ( $2\theta_{\text{max}} = 45^\circ$ ) with graphite-monochromatized Mo K $\alpha$  radiation ( $\lambda = 0.71073 \text{ \AA}$ ) at room temperature. The data were corrected for Lorentz, polarization, and absorption effects. The structures were solved by Patterson and Fourier methods and subsequently refined by full-matrix least-squares procedures using the NRCVAX program.<sup>15</sup> The weighting scheme is  $w = 1/\sigma^2(F_o)$ . The following details are given for each complex.

(12) Sayre, R. J. *Am. Chem. Soc.* **1955**, 6689.

(13) (a) Krause, R. A. *Inorg. Chim. Acta* **1977**, 22, 209. (b) Anderson, S.; Seddon, K. R. *J. Chem. Res., Synop.* **1979**, 74.

(14) Che, C. M.; Wong, K. Y.; Anson, F. C. *J. Electroanal. Chem. Interfacial Electrochem.* **1987**, 226, 211.

(15) Gabe, E. J.; LePage, Y.; Charland, J. P.; Lee, F. L.; White, P. S. *J. Appl. Crystallogr.* **1989**, 22, 384.

**Table 1.** Crystal Data Collection and Refinement Parameters for [Ru(bpy)(L-H)<sub>2</sub>][ZnBr<sub>4</sub>]·CH<sub>3</sub>CN and [Ru(L)(L-H)<sub>2</sub>]Cl<sub>2</sub>·2H<sub>2</sub>O

	[Ru(bpy)(L-H) <sub>2</sub> ][ZnBr <sub>4</sub> ]·CH <sub>3</sub> CN	[Ru(L)(L-H) <sub>2</sub> ]Cl <sub>2</sub> ·2H <sub>2</sub> O
empirical formula	[RuC <sub>22</sub> H <sub>38</sub> N <sub>6</sub> ][ZnBr <sub>4</sub> ]·CH <sub>3</sub> CN	[RuC <sub>18</sub> H <sub>46</sub> N <sub>6</sub> ]Cl <sub>2</sub> ·2H <sub>2</sub> O
fw	913.69	554.74
space group	<i>P</i> 2 <sub>1</sub> / <i>n</i>	<i>I</i> 4 <sub>1</sub> / <i>a</i>
<i>a</i> (Å)	12.597(2)	31.892(6)
<i>b</i> (Å)	15.909(2)	
<i>c</i> (Å)	16.785(2)	10.819(3)
$\beta$ (deg)	91.74(1)	
<i>V</i> (Å <sup>3</sup> )	3362.2 (8)	11003(3)
<i>Z</i>	4	16
$\mu$ (cm <sup>-1</sup> )	6.64	6.86
<i>D</i> <sub>calcd</sub> (g cm <sup>-3</sup> )	1.805	1.339
<i>R</i> <sup>a</sup>	0.033	0.055
<i>R</i> <sub>w</sub>	0.031	0.045
<i>F</i> (000)	1783	4704
GoF <sup>c</sup>	1.13	2.66

<sup>a</sup>  $R = \sum ||F_o| - |F_c|| / \sum |F_o|$ . <sup>b</sup>  $R_w = [\sum w^2(|F_o| - |F_c|)^2 / \sum w^2|F_o|^2]^{1/2}$ . <sup>c</sup>  $GoF = [\sum w(|F_o| - |F_c|)^2 / (n - p)]^{1/2}$ , where *n* = number of unique reflections used in structure refinement and *p* = number of variables in the least-squares refinement.

**[Ru(bpy)(L-H)<sub>2</sub>][ZnBr<sub>4</sub>]·CH<sub>3</sub>CN.** A yellow crystal of dimensions 0.05 × 0.30 × 0.35 mm was used for data collection. A total of 4374 unique reflections were measured, 2518 (*n*) of which had *I* > 2.0σ(*I*) and were used in structure refinement. The number of variables in the least-squares refinement was 335 (*p*). The final Fourier difference map showed extrema at -2.08 and +0.91 e Å<sup>-3</sup>.

**[Ru(L)(L-H)<sub>2</sub>]Cl<sub>2</sub>·2H<sub>2</sub>O.** A red crystal of dimensions 0.20 × 0.25 × 0.30 mm was used for data collection. A total of 3585 unique reflections were measured, 2479 (*n*) of which had *I* > 2.0σ(*I*) and were used in structure refinement. The number of variables in the least-squares refinement was 253 (*p*). The final Fourier difference map showed extrema at -0.71 and +0.91 e Å<sup>-3</sup>.

The atomic coordinates of non-hydrogen atoms are listed in Tables 2 and 3, and selected bond distances and angles are given in Table 4.

## Results and Discussion

The oxidation chemistry of high-valent ruthenium(IV)-amide complexes should be of considerable interest, but the reported examples with a monodentate amide ligand are sparse. In 1984, Keene and co-workers reported the preparation and crystal structure of [Ru<sup>IV</sup>(tpy)(bpy)(N=CMe<sub>2</sub>)](ClO<sub>4</sub>)<sub>3</sub> (tpy = 2,2':6',2''-terpyridine; bpy = 2,2'-bipyridine).<sup>5c</sup> Later, the isolation of the (diphenylamido)ruthenium(IV) porphyrin Ru(3,4,5-(MeO)<sub>2</sub>TPP)(NPh<sub>2</sub>)<sub>2</sub> (3,4,5-(MeO)<sub>2</sub>TPP = *meso*-tetrakis(3,4,5-trimethoxyphenyl)porphyrin dianion),<sup>5b</sup> which was characterized by <sup>1</sup>H NMR, IR, and UV-vis spectroscopy, was reported by Che and co-workers. In this work, oxidative deprotonation of [Ru<sup>II</sup>(bpy)(L)<sub>2</sub>]<sup>2+</sup> and the reaction of [Ru<sup>VI</sup>NCl<sub>4</sub>]<sup>-</sup> with L were found to give [Ru<sup>IV</sup>(bpy)(L-H)<sub>2</sub>]<sup>2+</sup> and [Ru<sup>IV</sup>(L)(L-H)<sub>2</sub>]<sup>2+</sup>, respectively.

Perspective views of the [Ru<sup>IV</sup>(bpy)(L-H)<sub>2</sub>]<sup>2+</sup> and [Ru<sup>IV</sup>(L)(L-H)<sub>2</sub>]<sup>2+</sup> cations are shown in Figures 1 and 2, respectively. The two complexes feature the first examples of bis(amido)ruthenium(IV). [Ru<sup>IV</sup>(L)(L-H)<sub>2</sub>]<sup>2+</sup> is isostructural with [Os<sup>IV</sup>(L)(L-H)<sub>2</sub>]<sup>2+</sup> reported by Ludi and co-workers.<sup>16</sup> The intriguing feature of the structures is the short Ru-N(amide) distances: Ru-N2 [1.856(7) Å] and Ru-N4 [1.856(6) Å] in [Ru<sup>IV</sup>(bpy)(L-H)<sub>2</sub>]<sup>2+</sup> and Ru-N3 [1.835(7) Å] and Ru-N5 [1.850(8) Å] in [Ru<sup>IV</sup>(L)(L-H)<sub>2</sub>]<sup>2+</sup>. These distances are comparable to the Ru(IV)-N(amide) distance of 1.831(10) Å in [Ru<sup>IV</sup>(tpy)(bpy)-

**Table 2.** Atomic Coordinates and Temperature Factors (Å<sup>2</sup>), with Standard Deviations in Parentheses, for Non-Hydrogen Atoms of [Ru(bpy)(L-H)<sub>2</sub>][ZnBr<sub>4</sub>]·CH<sub>3</sub>CN

	<i>x</i>	<i>y</i>	<i>z</i>	<i>B</i> <sub>eq</sub>
Ru	0.59130(5)	0.71318(4)	0.25595(4)	2.52(3)
N1	0.6411(5)	0.7620(4)	0.3681(4)	2.9(3)
N2	0.4823(5)	0.7890(4)	0.2728(4)	3.2(3)
N3	0.5115(5)	0.6587(4)	0.1558(4)	3.4(3)
N4	0.5521(5)	0.6108(4)	0.2991(4)	2.9(3)
N5	0.7555(5)	0.6696(4)	0.2428(4)	2.8(3)
N6	0.6681(5)	0.7989(4)	0.1750(4)	2.9(3)
C1	0.5840(7)	0.8413(5)	0.3874(5)	3.7(4)
C2	0.5868(8)	0.8548(6)	0.4789(5)	5.3(6)
C3	0.6436(8)	0.9144(6)	0.3484(6)	5.0(5)
C4	0.4716(7)	0.8289(5)	0.3510(5)	3.3(4)
C5	0.4095(8)	0.9117(6)	0.3413(6)	5.3(5)
C6	0.4033(7)	0.7692(6)	0.4014(5)	5.0(6)
C7	0.4775(6)	0.5533(5)	0.2573(5)	3.7(4)
C8	0.3657(8)	0.5774(6)	0.2825(6)	5.8(6)
C9	0.5001(8)	0.4622(6)	0.2837(6)	5.1(5)
C10	0.4941(7)	0.5667(5)	0.1660(5)	3.6(4)
C11	0.3978(8)	0.5400(6)	0.1151(6)	5.9(6)
C12	0.5934(8)	0.5215(6)	0.1379(5)	4.7(5)
C13	0.7975(7)	0.6075(5)	0.2870(5)	3.9(5)
C14	0.9034(7)	0.5878(5)	0.2875(6)	4.4(5)
C15	0.9689(7)	0.6320(6)	0.2415(6)	5.1(5)
C16	0.9285(6)	0.6975(5)	0.1958(5)	3.7(4)
C17	0.8209(6)	0.7151(5)	0.1994(5)	2.9(4)
C18	0.7682(6)	0.7851(5)	0.1565(4)	2.9(4)
C19	0.8190(7)	0.8324(6)	0.0980(5)	4.1(5)
C20	0.7616(8)	0.8940(6)	0.0590(5)	4.9(5)
C21	0.6587(8)	0.9069(6)	0.0748(5)	4.9(5)
C22	0.6130(7)	0.8574(5)	0.1337(5)	3.7(4)
Zn	0.73597(8)	0.14507(7)	0.92772(6)	3.36(5)
Br1	0.89802(7)	0.09875(6)	0.99484(5)	3.75(4)
Br2	0.78172(8)	0.23141(7)	0.81637(6)	5.24(6)
Br3	0.63512(8)	0.02530(6)	0.88423(6)	4.53(5)
Br4	0.63223(8)	0.23283(8)	1.01278(6)	5.52(6)
N7	0.3377(7)	0.3282(5)	0.9960(5)	6.5(5)
C23	0.3589(8)	0.2854(7)	1.0465(6)	5.7(6)
C24	0.3853(9)	0.2288(9)	1.1116(7)	9.3(8)

(N=CMe<sub>2</sub>)](ClO<sub>4</sub>)<sub>3</sub><sup>5c</sup> and the Os(IV)-N(amide) distances of 1.880(6) Å in [Os<sup>IV</sup>(L)(L-H)<sub>2</sub>]<sup>2+</sup> and 1.896(7) Å in [Os<sup>IV</sup>(en)(en-H)<sub>2</sub>]<sup>2+</sup> (en = ethane-1,2-diamine).<sup>17</sup> They are, however, shorter than the Ru(IV)-N(amide) distances [1.987-2.044(5) Å] in [Ru(chbae)(PPh<sub>3</sub>)(py)] (H<sub>4</sub>chbae = 1,2-bis(3,5-dichloro-2-hydroxybenzamido)ethane; py = pyridine),<sup>5a</sup> in which the coordinated amide is part of the chelating ligand. The N2-Ru-N4 angle of 107.7(3)° in [Ru<sup>IV</sup>(bpy)(L-H)<sub>2</sub>]<sup>2+</sup> and the N3-Ru-N5 angle of 110.3(4)° in [Ru<sup>IV</sup>(L)(L-H)<sub>2</sub>]<sup>2+</sup> are significantly larger than the *cis*-N(amine)-Ru-N(amide/amine) angles (for example, N2-Ru-N3 = 92.9(3)° and N1-Ru-N4 = 92.9(3)° in [Ru<sup>IV</sup>(bpy)(L-H)<sub>2</sub>][ZnBr<sub>4</sub>] and N2-Ru-N3 = 88.4(3)° and N4-Ru-N5 = 94.9(3)° in [Ru<sup>IV</sup>(L)(L-H)<sub>2</sub>]Cl<sub>2</sub>). These angles are also comparable to the O=Ru=O bond angles in some *cis*-dioxoruthenium(VI) complexes such as that of 112.0(4)° in *cis*-[Ru<sup>VI</sup>(Tet-Me<sub>6</sub>)(O)<sub>2</sub>]<sup>2+</sup> (Tet-Me<sub>6</sub> = *N,N,N',N'*,3,6-hexamethyl-3,6-diazaoctane-1,8-diamine).<sup>18</sup> This suggests a significant repulsive interaction between the two Ru-N(amide) bonds, which are in a *cis* configuration. In [Ru<sup>IV</sup>(L)(L-H)<sub>2</sub>]<sup>2+</sup>, the two Ru-N(amide) bonds show a *trans* effect. The two Ru-N(amine) bonds *trans* to it are elongated by an average of 0.09 Å compared with the elongation of Os-N(amine) bonds by 0.04 Å in [Os<sup>IV</sup>(L)(L-H)<sub>2</sub>]<sup>2+</sup> and 0.08 Å in [Os<sup>IV</sup>(en)(en-H)<sub>2</sub>]<sup>2+</sup>.<sup>17</sup> The *trans* effect also results the elongation of the Ru-N(bpy) bonds in [Ru<sup>IV</sup>(bpy)(L-H)<sub>2</sub>]<sup>2+</sup> (2.199(6) and 2.172(6) Å), which

(16) Patel, A.; Ludi, A.; Bürgi, H.-B.; Raselli, A.; Bigler, P. *Inorg. Chem.* **1992**, *31*, 3405.

(17) Lay, P. A.; Sargeson, A. M.; Skelton, B. W.; White, A. H. *J. Am. Chem. Soc.* **1982**, *104*, 6161.

(18) Li, C. K.; Che, C. M.; Tong, W. F.; Tang, W. T.; Wong, K. Y.; Lai, T. F. *J. Chem. Soc., Dalton Trans.* **1992**, 2109.

**Table 3.** Atomic Coordinates and Temperature Factors ( $\text{\AA}^2$ ), with Standard Deviations in Parentheses, for Non-Hydrogen Atoms of  $[\text{Ru}(\text{L})(\text{L}-\text{H})_2]\text{Cl}_2 \cdot 2\text{H}_2\text{O}$ 

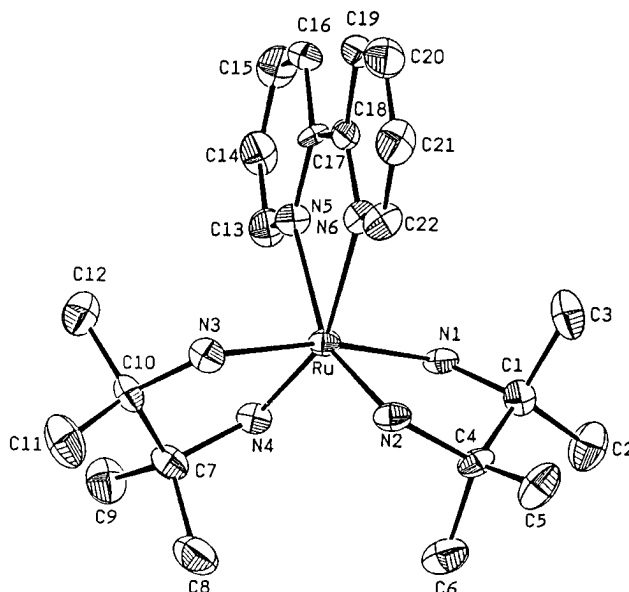
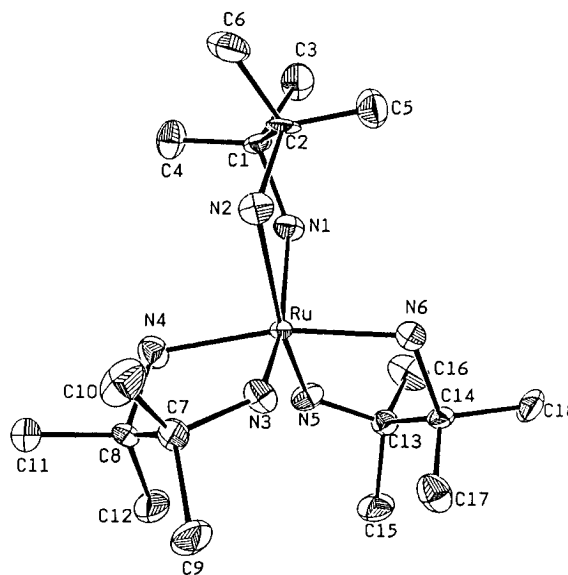
	<i>x</i>	<i>y</i>	<i>z</i>	<i>B</i> <sub>eq</sub>
Ru	0.13372(2)	0.63996(2)	0.05735(7)	2.26(3)
Cl1	0.14025(11)	0.75778(9)	0.9206(3)	6.57(19)
Cl2	0.26917(9)	0.6217(1)	0.8958(3)	7.03(20)
N1	0.1153(3)	0.6537(2)	-0.1328(7)	4.3(5)
N2	0.1630(2)	0.5922(2)	-0.0577(8)	4.4(4)
N3	0.1602(2)	0.6168(2)	0.1915(8)	4.2(4)
N4	0.1899(3)	0.6732(3)	0.0621(8)	5.0(5)
N5	0.1009(3)	0.6849(2)	0.1059(7)	4.5(4)
N6	0.0754(2)	0.6119(2)	0.0895(8)	4.4(4)
C1	0.1388(3)	0.6311(3)	-0.2343(8)	3.4(5)
C2	0.1460(3)	0.5859(3)	-0.1852(8)	4.0(5)
C3	0.1114(4)	0.6301(4)	-0.3505(10)	6.9(8)
C4	0.1770(3)	0.6542(3)	-0.2656(10)	5.6(6)
C5	0.1100(3)	0.5596(3)	-0.1831(12)	6.0(7)
C6	0.1813(4)	0.5638(3)	-0.2577(11)	6.7(7)
C7	0.2013(3)	0.6285(3)	0.2400(9)	4.7(6)
C8	0.2076(3)	0.6743(3)	0.1921(9)	4.9(6)
C9	0.1972(4)	0.6280(5)	0.3827(10)	8.1(9)
C10	0.2350(4)	0.5980(4)	0.2051(12)	7.8(8)
C11	0.2542(4)	0.6853(4)	0.1853(12)	8.4(8)
C12	0.1841(4)	0.7079(4)	0.2628(12)	8.4(8)
C13	0.0571(3)	0.6819(3)	0.1453(9)	3.9(5)
C14	0.0506(3)	0.6362(3)	0.1861(9)	4.4(5)
C15	0.0521(4)	0.7135(4)	0.2511(11)	7.0(7)
C16	0.0293(4)	0.6959(4)	0.0397(12)	7.5(8)
C17	0.0664(3)	0.6274(3)	0.3119(11)	5.9(7)
C18	0.0054(3)	0.6221(5)	0.1765(10)	7.7(8)
O1	0.2379(5)	0.2664(6)	0.0474(17)	27.4(8)
O2	0.0326(7)	0.5195(7)	0.0605(25)	40.4(13)

**Table 4.** Selected Bond Distances ( $\text{\AA}$ ) and Bond Angles (deg) for  $[\text{Ru}(\text{bpy})(\text{L}-\text{H})_2][\text{ZnBr}_4] \cdot \text{CH}_3\text{CN}$  and  $[\text{Ru}(\text{L})(\text{L}-\text{H})_2]\text{Cl}_2 \cdot 2\text{H}_2\text{O}$ 

$[\text{Ru}(\text{bpy})(\text{L}-\text{H})_2][\text{ZnBr}_4] \cdot \text{CH}_3\text{CN}$			
Ru-N1	2.114(6)	N2-C4	1.468(10)
Ru-N2	1.856(7)	N3-C10	1.490(10)
Ru-N3	2.118(6)	N4-C7	1.473(10)
Ru-N4	1.856(6)	N5-C13	1.335(10)
Ru-N5	2.199(6)	N5-C17	1.330(10)
Ru-N6	2.172(6)	N6-C18	1.327(10)
N1-C1	1.49(1)	N6-C22	1.342(10)
N1-Ru-N2	80.0(3)	N3-Ru-N5	102.5(3)
N1-Ru-N3	167.9(3)	N3-Ru-N6	88.3(2)
N1-Ru-N4	92.9(3)	N4-Ru-N5	91.4(3)
N1-Ru-N5	87.2(2)	N4-Ru-N6	157.5(3)
N1-Ru-N6	101.6(2)	N5-Ru-N6	72.4(2)
N2-Ru-N3	92.9(3)	Ru-N1-C1	111.8(4)
N2-Ru-N4	107.7(3)	Ru-N2-C4	120.4(5)
N2-Ru-N5	157.4(3)	Ru-N3-C10	112.3(5)
N2-Ru-N6	91.9(3)	Ru-N4-C7	122.2(5)
N3-Ru-N4	79.9(3)		
$[\text{Ru}(\text{L})(\text{L}-\text{H})_2]\text{Cl}_2 \cdot 2\text{H}_2\text{O}$			
Ru-N(1)	2.184(8)	N(1)-C(1)	1.513(12)
Ru-N(2)	2.178(8)	N(2)-C(2)	1.496(12)
Ru-N(3)	1.835(7)	N(3)-C(7)	1.458(12)
Ru-N(4)	2.083(8)	N(4)-C(8)	1.516(13)
Ru-N(5)	1.850(8)	N(5)-C(13)	1.463(12)
Ru-N(6)	2.093(8)	N(6)-C(14)	1.523(12)
N(1)-Ru-N(2)	73.6(3)	N(3)-Ru-N(4)	77.8(3)
N(1)-Ru-N(3)	161.8(3)	N(3)-Ru-N(5)	110.3(4)
N(1)-Ru-N(4)	98.8(3)	N(3)-Ru-N(6)	96.1(3)
N(1)-Ru-N(5)	87.7(3)	N(4)-Ru-N(5)	94.9(3)
N(1)-Ru-N(6)	90.2(3)	N(4)-Ru-N(6)	167.9(3)
N(2)-Ru-N(3)	88.4(3)	N(5)-Ru-N(6)	77.3(3)
N(2)-Ru-N(4)	90.1(3)	Ru-N(3)-C(7)	126.5(6)
N(2)-Ru-N(5)	161.2(3)	Ru-N(5)-C(13)	125.0(6)
N(2)-Ru-N(6)	100.2(3)		

are longer than the Ru-N(bpy) distances of 2.076(7) and 2.055-(6)  $\text{\AA}$  in  $[\text{Ru}^{\text{IV}}(\text{tpy})(\text{bpy})(\text{N}=\text{CMe}_2)](\text{ClO}_4)_3 \cdot 5\text{c}$

Complexes 2-7 are diamagnetic, and the NMR spectrum of

**Figure 1.** Perspective view of the  $[\text{Ru}(\text{bpy})(\text{L}-\text{H})_2]^{2+}$  cation.**Figure 2.** Perspective view of the  $[\text{Ru}(\text{L})(\text{L}-\text{H})_2]^{2+}$  cation.

4 is shown in Figure 3. Both 4 and 7 show very low field  $^1\text{H}$  signals at  $\delta$  13.16 and 12.31 ppm, respectively, and these are assigned to the amido protons. The much downfield chemical shift is attributed to the strong  $d\pi-p\pi$  interaction between N(amide) and ruthenium atoms. The highly electrophilic ruthenium(IV) would compete with the N(amide) atoms for the bonded electron(s), thus rendering the N(amide) atoms to be very electrophilic and hence leading to the downfield shift of the amide protons and the quaternary carbons attached to it.

Both complexes 4 and 7 are air-stable solids, despite having two amido groups *cis* to each other. They are isostructural with  $[\text{Os}(\text{L})(\text{L}-\text{H})_2]^{2+}$ <sup>16</sup> and  $[\text{Os}(\text{en})(\text{en}-\text{H})_2]^{2+}$ ,<sup>17</sup> in which the two amide groups are in different chelate ligands. Since the preferred angle between the two *cis* Ru-N(amide) bonds is  $107-110^\circ$  from crystal structure analysis, severe angular strain would result if the two amide moieties were in the same chelate. In previous work, the electrogenerated  $[\text{Ru}^{\text{IV}}(\text{bpy})_2(\text{L}-3\text{H})]^{2+}$  ( $\text{L}-3\text{H} = (\text{HNCMe}_2\text{CMe}_2\text{N})^{3-}$ ) had large angular strain in the chelate, leading to C-C bond cleavage of the ligand L and formation of  $[\text{Ru}^{\text{II}}(\text{bpy})_2(\text{HN}=\text{CMe}_2)_2]^{2+}$ .<sup>6b</sup>

Like  $[\text{Ru}^{\text{II}}(\text{bpy})_2(\text{L})]^{2+}$ <sup>6b</sup> and *trans*- $[\text{Os}^{\text{III}}(\text{L})_2\text{Cl}_2]^+$ ,<sup>10</sup> both  $[\text{Ru}^{\text{II}}(\text{bpy})(\text{L})_2]^{2+}$  and  $[\text{Ru}^{\text{IV}}(\text{L})(\text{L}-\text{H})_2]^{2+}$  undergo reversible

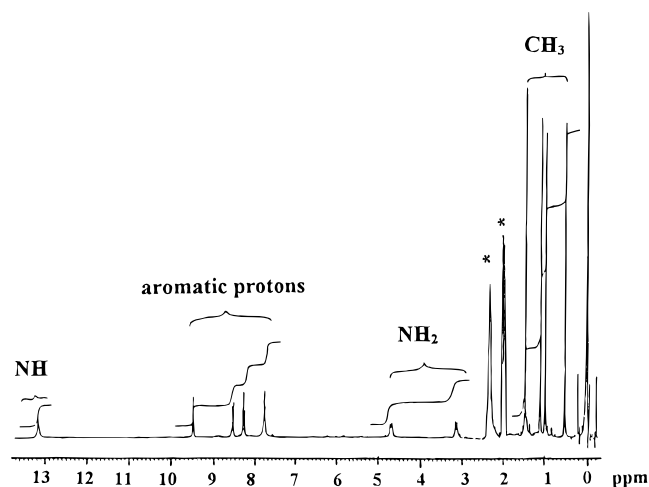


**Figure 3.**  $^1\text{H}$  NMR spectrum of  $[\text{Ru}(\text{bpy})(\text{L}-\text{H})_2]^{2+}$  in  $\text{CD}_3\text{CN}$ . Asterisks denote resonances due to partially deuterated solvent and  $\text{H}_2\text{O}$ .

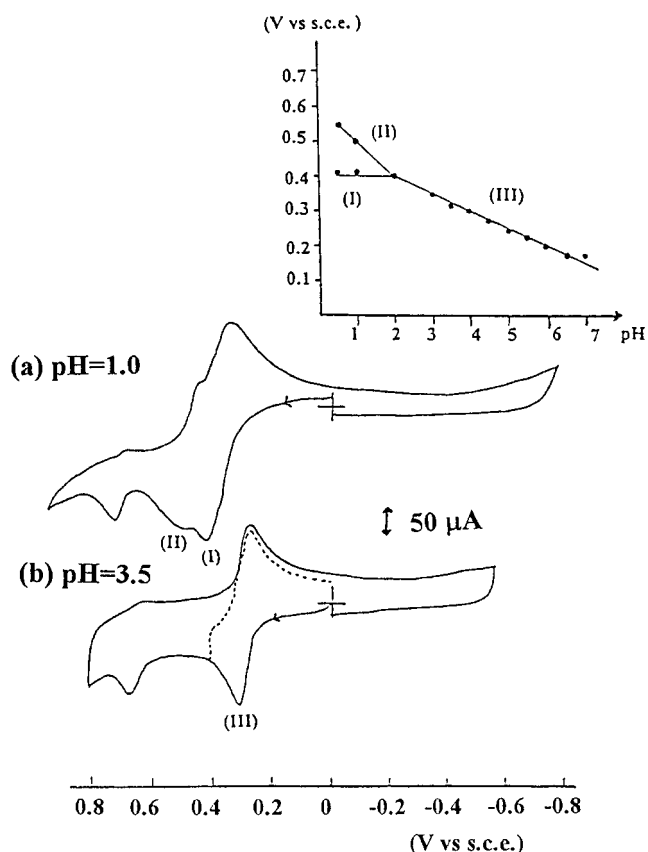


**Figure 4.** Cyclic voltammograms of  $[\text{Ru}^{\text{II}}(\text{bpy})(\text{L})_2](\text{PF}_6)_2$  in aqueous solution: (a)  $\text{pH} = 1.0$ ; (b)  $\text{pH} = 3.5$ . Conditions: working electrode, edge plane pyrolytic graphite; scan rate, 20 mV/s. Inset: pH dependence of  $E_{\text{pa}}$  for (I), (II), and (III).

proton-coupled electron-transfer reactions. The cyclic voltammograms of  $[\text{Ru}^{\text{II}}(\text{bpy})(\text{L})_2]^{2+}$  in aqueous solution of different pHs are identical to that of  $[\text{Ru}^{\text{IV}}(\text{bpy})(\text{L}-\text{H})_2]^{2+}$  recorded under similar conditions. Sample voltammograms are shown in Figure 4.

In 0.1 M  $\text{CF}_3\text{COOH}$ , there are two reversible couples with  $E_{1/2} = 0.38$  V (I) and 0.46 V (II) and an irreversible oxidative wave with  $E_{\text{pa}} = 0.72$  V vs SCE. At  $\text{pH} \geq 2.0$ , the two reversible couples merge to form a new reversible two-electron couple (III), which becomes irreversible at  $\text{pH} \geq 4.0$ . Couple (I) is pH-independent whereas the  $E_{1/2}$  of (II) shifts cathodically by 110 mV/pH unit in the pH range 0.5–2.0. The  $E_{\text{pa}}$  of (III) shifts cathodically by 55 mV/pH unit in the pH range 2–7. The

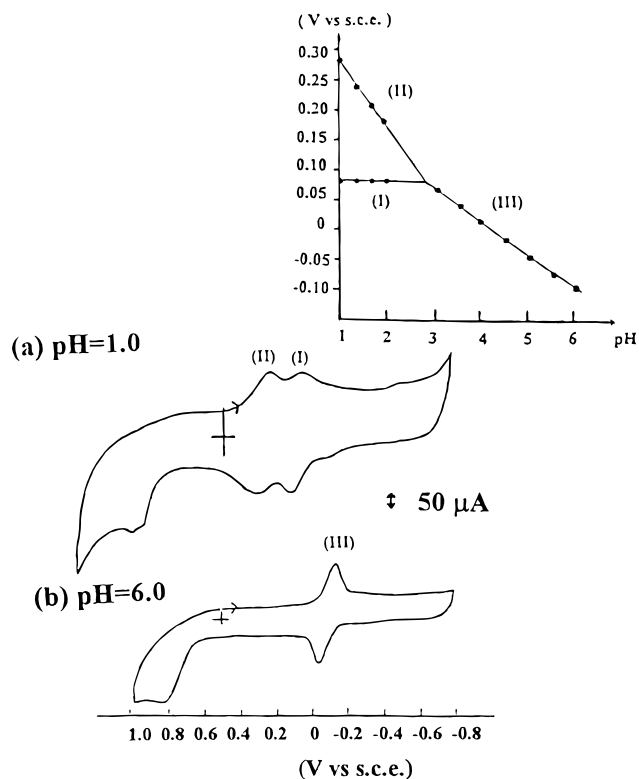
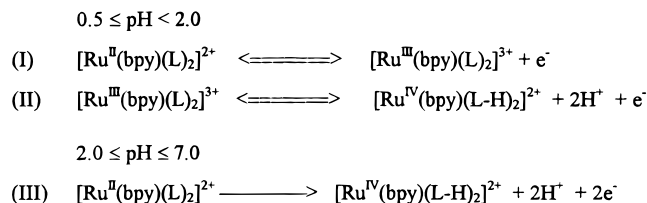


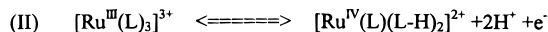
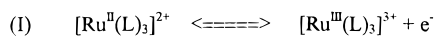
**Figure 5.** Cyclic voltammograms of  $[\text{Ru}^{\text{IV}}(\text{L})(\text{L}-\text{H})_2]\text{Cl}_2$  in aqueous solution: (a)  $\text{pH} = 1.0$ ; (b)  $\text{pH} = 6.0$ . Conditions: working electrode, edge plane pyrolytic graphite; scan rate, 100 mV/s. Inset: pH dependence of  $E_{1/2}$  of (I), (II), and (III).

pH dependences of the  $E_{\text{pa}}$  of (I), (II), and (III) are given in the inset of Figure 4. Controlled-potential coulometry of  $[\text{Ru}^{\text{II}}(\text{bpy})(\text{L})_2]^{2+}$  at 0.60 V vs SCE in 0.1 M  $\text{CF}_3\text{COOH}$  established  $n = 2.0$ , and the oxidized product is  $[\text{Ru}^{\text{IV}}(\text{bpy})(\text{L}-\text{H})_2]^{2+}$ . On the basis of the above electrochemical results, the following electrode reactions are assigned:

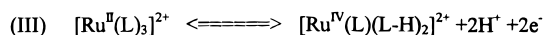


$[\text{Ru}^{\text{IV}}(\text{L})(\text{L}-\text{H})_2]^{2+}$  displays electrochemistry similar to that of  $[\text{Ru}^{\text{II}}(\text{bpy})(\text{L})_2]^{2+}$  except that the redox couples are more reversible at high pH. Its cyclic voltammograms at pH 1.0 and 6.0 are shown in Figure 5. The same cyclic voltammograms have also been recorded with  $[\text{Ru}(\text{L})_3]^{2+}$  under identical conditions. In 0.1 M  $\text{CF}_3\text{COOH}$  ( $\text{pH} = 1.0$ ), there are two reversible couples: (I) at  $E_{1/2} = 0.09$  V and (II) at  $E_{1/2} = 0.29$  V vs SCE. Both couples have a  $\Delta E_{\text{p}}$  of 58 mV and an  $i_{\text{pa}}/i_{\text{pc}}$  ratio of 0.9 at a scan rate of 100 mV  $\text{s}^{-1}$ . There is also one irreversible oxidative wave with  $E_{\text{pa}} = 1.0$  V vs SCE. Couple (I) is pH-independent whereas the  $E_{1/2}$  of couple (II) shifts cathodically by 110 mV/pH unit at pH 1–3. At  $\text{pH} \geq 3.0$ , the two couples merge to form a new reversible couple (III), the  $E_{1/2}$  of which shifts cathodically by 55 mV/pH unit at pH 3.0–6.0. The pH dependence of the  $E_{1/2}$  of couples (I), (II), and (III) (inset of Figure 5) suggests the following electrode reactions:

$$1.0 \leq \text{pH} < 3.0$$



$$3.0 \leq \text{pH} \leq 6.0$$



The  $E_{\text{pa}}$  of the irreversible oxidative wave also shows pH dependence, shifting to the cathodic side with increase in pH. For example, the  $E_{\text{pa}}$  is 1.0 V at pH 1.0 and 0.81 V at pH 6.0. Presumably, the irreversible oxidative wave is due to the oxidation of  $[\text{Ru}^{\text{IV}}(\text{L})(\text{L}-\text{H})_2]^{2+}$  to some high-valent Ru(V)- or Ru(VI)-imido species which are unstable. Attempts to isolate the oxidized species were unsuccessful.

A direct comparison of the electrochemical data of **3** and **7** reveals some interesting results. The replacement of one bipyridine with a saturated chelating amine ligand L lowers the  $E_{1/2}$  of the Ru(III)-amine/Ru(II)-amine and Ru(IV)-amide/Ru(III)-amine couples by 290 and 170 mV, respectively. Similar changes in redox potentials have previously been reported in Ru=O chemistry. The larger cathodic shift of  $E_{1/2}$  for the Ru(III)-amine/Ru(II)-amine complexes than for the Ru(IV)-amide/Ru(III)-amine couples from **3** to **7** is attributed to the metal to ligand back-bonding of Ru(II) with bipyridine ligand. However, the extent of the back bonding is insignificant in Ru(III) complexes, and so the cathodic shift of  $E_{1/2}$  for the

Ru(IV)-amide/Ru(III)-amine couple is smaller when one bipyridine is replaced by ligand L.

### Conclusion

Electrochemical studies of  $[\text{Ru}^{\text{II}}(\text{bpy})(\text{L})_2]^{2+}$  and  $[\text{Ru}^{\text{IV}}(\text{L})(\text{L}-\text{H})_2]^{2+}$  show that primary amine ligands without  $\alpha$ -CH groups are able to prohibit oxidative dehydrogenation reaction(s) of coordinated amine ligands. As a result, high-valent ruthenium-amido complexes, which are stabilized by  $d\pi$ - $p\pi$  interactions, could be isolated. The present work highlights the probability that the redox chemistry of ruthenium-amido complexes could be as rich as that of the Ru=O species. A compilation of the  $E^\circ$  values of various metal-imido/metal-amine and metal-amido/metal-amine couples is essential to the future study of metal-nitrogen multiple bonding.

**Acknowledgment.** We acknowledge support from The University of Hong Kong and The Hong Kong Research Grant Council.

**Supporting Information Available:** Tables of isotropic thermal parameters and calculated positional parameters for hydrogen atoms, crystal data and refinement parameters, and complete bond distances and angles for  $[\text{Ru}(\text{bpy})(\text{L}-\text{H})_2][\text{ZnBr}_4] \cdot \text{CH}_3\text{CN}$  and  $[\text{Ru}(\text{L})(\text{L}-\text{H})_2]\text{Cl}_2 \cdot 2\text{H}_2\text{O}$  (5 pages). Ordering information is given on any current masthead page.

IC951145N